Powder Technology 245 (2013) 21–27

Contents lists available at SciVerse ScienceDirect

Powder Technology

journal homepage: www.elsevier.com/locate/powtec

Design of ceramic paste formulations for co-extrusion

Jonathan Powell [a,*], Suttichai Assabumrungrat [b], Stuart Blackburn [c]

[a] School of Chemical Engineering and Advanced Materials, Newcastle University, UK
[b] Department of Chemical Engineering, Faculty of Engineering, Chulalongkorn University, Bangkok 10330, Thailand
[c] School of Chemical Engineering, The University of Birmingham, UK

ARTICLE INFO

Article history:
Received 15 November 2012
Received in revised form 1 April 2013
Accepted 15 April 2013
Available online 22 April 2013

Keywords:
Co-extrusion
Paste
Slip flow

ABSTRACT

The rheological and flow behaviour of ceramic pastes with varying solids loadings (solids volume fraction) has been studied. The pastes were shown to exhibit power law slip flow at both low and high solids loadings, with no slip yield stress. As would be expected, the extrusion rheometry data showed an increase in the die entry extrusion pressures with solids loading, in a trend similar to that of the Dougherty–Krieger equation. The die land flow however was shown to exhibit, only within a narrow range of solids loadings of approximately 53 to 56 v/v %, a trend in the die land extrusion pressure that was relatively independent of solids loading. Outside of this range the die land extrusion pressures increased significantly with solids loading in a trend similar to that of the die entry pressures. Using the Mooney analysis method, this was shown to be due to the development of slip flow with solids loading, as is consistent with other studies into the flow behaviour of concentrated suspensions. The slip velocity was also shown to be related to the wall shear stress by way of power law relationship also consistent with results from previous studies of concentrated suspensions using shear thinning liquid phases. The results presented in this report show that by using paste formulations that lie within said range of solids loadings, improved plug flow can be achieved in the die land without a significant change in the die land extrusion pressure at a given flow rate. This offers an advantage in the co-extrusion of ceramic products such as micro-tubular solid oxide fuel cells, as a uniform velocity profile results in improved control of the laminate structure.

1. Introduction

The co-extrusion of multiple pastes into a single extrudate requires the fine tuning and unification of the paste rheologies in order to prevent the formation of flow defects in a continuous or semi-continuous extrusion process. This requires the formulation of individual pastes with consideration of effects due to particle size, size distribution, morphology and surface chemistry, as well as pore size, distribution and shape. Previous work by Liang and Blackburn [1,2], Zhang et al. [3], Chen et al. [4], Powell and Blackburn [5,6] and others have looked at the co-extrusion of multi-layered tubes. The tubes were relatively large, with layer thicknesses being in the order of 1 mm, a limitation which could be overcome by a change in design of the co-extrusion process and equipment. Some of these authors also reported the formation of delamination defects, which again can be overcome by improved design of the co-extruder [5,6]. This paper follows on from two previous publications by the same authors [5,6] which presented the results of an investigation into the manufacture of multi-layered ceramic micro-tubes that could be used in the manufacture of solid oxide fuel cells.

When co-extruding pastes into laminate structures, it is preferable to achieve a uniform velocity profile across the co-extrudate, such that the velocities of the laminate layers are equal. By obtaining a uniform velocity profile which is relatively independent of the extrudate velocity, it is possible to have a co-extrusion process where the laminate structure of the co-extrudate is well controlled and relatively independent of the extrudate velocity and time. Uniform velocity profiles are achieved by designing the paste rheology to include a yield stress and slip or apparent slip at the wall.

The die land flow of ceramic pastes has been shown to be influenced by apparent slip at the wall [7–11], which in turn is influenced by the wall shear stress and solids loading of the paste. Unlike true wall slip where the velocity of the fluid at the wall is greater than zero, in paste flow the exclusion or depletion of solid particles from the wall results in the formation of a lubricating layer where this liquid itself has a die wall velocity of zero.

For extruding 'hard' sphere pastes with a high Peclet number ($Pe \gg 100$) [12] slip occurs at low solids loadings (~45%) [13] as well as high solids loadings (>50%) [14], but with increasing solids loading, slip flow becomes increasingly dominant [12,13]. Ballesta et al. have shown that for hard sphere colloidal suspensions, slip occurs for both low and high concentration suspensions but is shown to be much

* Corresponding author. Tel.: +44 65 96255366.
E-mail address: jdapowell@hotmail.com (J. Powell).

0032-5910
http://dx.doi.org/10.1016/j.powtec.2013.04.017

more significant for pastes with high solids loadings whereby the powder particles arrange themselves into a glass like structure [15].

For colloidal suspensions, with increasing Peclet number the depletion of solids from the wall and hence slip become increasingly important due to hydrodynamic effects [16]. For colloidal suspensions with low Peclet numbers where Brownian motion has a more significant role, slip has been shown to not take place at low solids loadings [17] as result of Brownian motion that hinders depletion of the solids from the die wall. For high solids loadings however, the particles crowd and lock in place reducing the extent to which the particle Brownian motion disturbs the slip layer. The transition to a solid like rheology where particles are locked together is therefore associated with an increase in slip flow [12].

This paper is part of study which investigated the influence of various formulation and processing variables on paste rheology, with the aim of unifying the rheology of 6 pastes. These variables included powder composition (three components NiO, YSZ and C), powder packing density, binder chemistry (water or cyclohexanone based), binder volume content in the paste and paste mixing method. Pastes made under these differing conditions and formulations were tested extrusion rheometry. This paper focusses on the effect of solids loading on the paste rheology and extrusion pressures, where the Benbow–Bridgwater model [18] as well as the Mooney analysis method is used to analyse the flow behaviour of pastes. Results presented include those from pastes mixed using two different mixing methods. The purpose of this is due to a limitation of the twin roll mill which only allows pastes with a narrow range of solids loadings to mixed, but also provides the benefit of emphasising that the observed trend in paste rheology with solids loading was independent on the mixing history of the pastes.

2. Materials

The ceramic pastes used for the rheological studies reported in this paper were made using 8 mol% yttria stabilised zirconia powder (YSZ) as the solid phase, HSY8 (Daiichi Kigenso Kagaku Kogyo Co., Japan), with a mean particle size of 0.5 μm, which is used to fabricate solid oxide fuel cell electrolytes. For the liquid phase of the paste, a proprietary binder system was used (Functional Materials Group, University of Birmingham, UK). This binder system is highly viscous in order to prevent phase migration during the extrusion process and to improve the stability of the paste. The viscosity was measured using a TA instruments AR500 rotational rheometer with a cone and plate geometry and was found to have a shear viscosity of 90 Pa.s at a shear rate of 2 s^{-1}. The constituents of the binder phase are provided in Table 1. Further details regarding the constituents cannot be provided as this is a proprietary formulation;

3. Methods

3.1. Paste Preparation

Prior to mixing the YSZ powder was dried in an oven at 120 °C overnight and stored in a desiccator to be cooled to room temperature. For both the twin roll mixing and the z-blade mixing, all the powders, which included the oxide, the stearic acid and the polyvinyl butyral, were dry mixed prior to adding the liquids.

Table 1
Binder formulation.

Constituents	Mass (g)
Cyclohexanone	25.50
Polyvinyl butyral	22.50
Stearic acid	0.45
Dibutyl phthalate	0.90

The density of the binder made according to the formulation given in Table 1 was measured using a constant volume pycnometer (Accupyc 1330, Micromeritics, UK) and was found to be 1835 $kg.m^{-3}$. This indicates that the constituents, PVB, DBP and stearic acid dissolve into the cylcohexanone with an insignificant increase in volume of the cyclohexanone — where the density of the binder, calculated based upon the assumption there is no volume change in the cyclohexanone with the addition of the other components, is 1840 $kg.m^{-3}$ — therefore the volume of the binder added to each paste was taken as the exact volume addition of cyclohexanone.

The volume fraction of solids in the pastes produced using the twin roll mill and z-blade mixer are provided in Table 2.

For the purpose of checking the liquid volume fraction of the pastes after mixing, the volume content of two twin mill rolled pastes not containing dibutyl phthalate and with solids loadings of 52.10% and 55.40% were checked by measuring the change in mass before and after drying over night at 120 °C. The calculated volume fractions were in agreement with the volume measured into the mixture which had an associated estimated error of ± 50 mm^3.

3.1.1. Twin roll milling

The twin roll milled pastes were mixed using a Bra bender Polymix, connected to a refrigeration unit for temperature control of the rollers. The rollers were kept at a temperature of 15 °C and so prior to the addition of material to the rollers condensation was removed with a long fibre cloth (long fibres were used in order to prevent contamination of the paste with fibres). The slow roller rotated at a fixed frequency of 27 min^{-1} and both rollers have a diameter of 50 mm.

The twin roll milled pastes, which were made of the solid YSZ powder and the liquid binder, were made with solids volume fractions (solids loadings) of 0.522, 0.525, 0.535, 0.545 and 0.554. The values 0.522 and 0.554 represent the range of solids loadings that could be made on the twin roll mills. At higher solids loadings the paste became brittle and no longer adhered to the rollers. At lower solids loadings the paste would adhere to both rollers rather than to the roller that rotates at a slightly higher rate, as intended, and would also fail to form a sheet of paste.

The material was mixed for a total of 12 min and added gradually during the first 5 min, ensuring that for each addition of material, the mixture was well homogenised. During this period of incrementally adding and mixing the paste, the rollers spacing was incrementally increased from 1 to 4 mm. Having added the complete mixture, the paste was repeatedly passed through the mixer, not allowing the paste to adhere to the rollers, with the rollers set at a spacing of 0.1 mm, to ensure all powder agglomerates were dispersed and the paste well homogenised.

3.1.2. z-blade mixing

For the purposes of consistency in the experimental method the powders and liquids were premixed as previously described and this mixture was then added to the z-blade mixer for a total of 4.5 h

Table 2
Composition of solid constituents as percentage volume and mass for z-blade and twin roll mill mixed pastes containing $(26.97 \pm 0.05) \times 10^{-6}$ m^3 of binder.

	HSY8 mass (g)	% w/w of solids	HSY8 vol (cm^3)
z-blade	88.97	64.32	14.58
	175.38	78.04	28.75
	205.16	80.61	33.63
	211.07	81.05	34.60
Twin roll mill	179.64	78.45	29.45
	181.82	78.65	29.81
	189.26	79.32	31.03
	197.04	79.97	32.30
	204.33	80.55	33.50

inside a small sealed unit, kept cool using a supply of cold tap water through a cooling jacket. Such a long mixing period was used as this was the minimum period required to form a paste from the formulation with the highest solids loading. The material was intermittently removed from the sides of the mixing bowl and the blades to ensure thorough mixing. All pastes were left to equilibrate for an hour after mixing before extrusion.

A wider range of solids loadings could be manufactured using the z-blade mixer as the mixing mechanism of this equipment is less sensitive to this variable. The pastes produced using this mixer, were made to solids loadings of 0.351, 0.516, 0.555, 0.562. At solids loadings higher than this it was not possible to form a paste.

3.2. Extrusion rheometry and rheological characterisation

A range of pastes, with varying solids loadings were rheologically characterised using a ram extrusion rheometer driven by a universal load frame. A 20.3 mm diameter barrel was fitted with interchangeable dies, each with a die entry angle of 90°. The ceramic pastes were extruded through dies with one of three diameters, 4, 6 and 8 mm. All dies of a given diameter came with three length/diameter (L/D) ratios; 1:1, 1:4 and 1:8. For each die geometry, the pastes were extruded at six extrudate velocities; 5.00, 2.00, 1.00, 0.50, 0.25 and 0.13 mm.s^{-1}. The extrusion pressures were calculated as the average values from data gathered over a ram displacement of at least 5 mm.

The pastes were rheologically characterised using the Benbow–Bridgwater six paste parameter equation [18];

$$P = P_1 + P_2 = 2(\sigma_0 + \alpha V_{ext}^m)\ln\left(\frac{D_0}{D}\right) + 4\frac{L}{D}(\tau_0 + \beta V_{ext}^n) \quad 1$$

where V_{ext} denotes the extrudate velocity, P represents the extrusion pressure, P_1 and P_2 represent the pressure drop due to die entry and die land flow, respectively. σ_0, α and m denote the yield stress, velocity coefficient and velocity exponent respectively, for die entry flow. τ_0 represents the die wall yield stress and β and n represent the die land flow velocity factor and exponent.

The die entry parameters were calculated from the die entry pressure which is obtained from a Bagley plot (extrusion pressure versus L/D) (Fig. 1). Extrapolating a linear plot at a given velocity back to the y-axis, the extrusion pressures for a die land length of zero (die entry pressure, P_1) are obtained. The die entry parameters were then obtained by fitting a three parameter power law curve to a plot of P_1 versus extrudate velocity, V_{ext}. Likewise the die land parameters were obtained from a plot of P_2 versus V_{ext}.

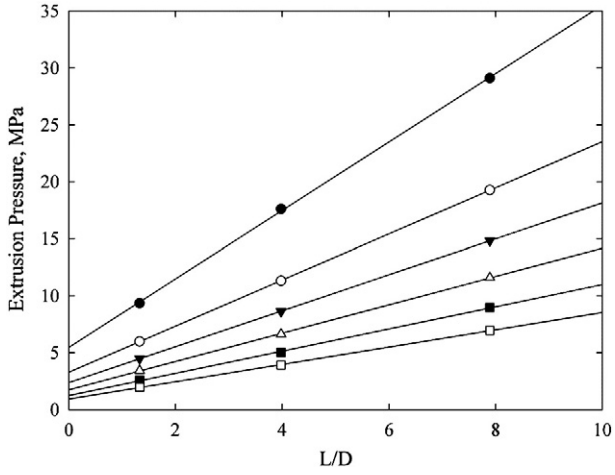

Fig. 1. Typical Bagley plot of extrusion data.

The Benbow–Bridgwater equation assumes that extrusion pastes undergo complete slip flow in the die land i.e. the slip and the extrudate velocities are equal. The applicability of this model to the pastes used in this study is assessed by means of a Mooney analysis and the change in extrusion pressures with solids loading.

3.3. Mooney analysis

The Mooney analysis method [9,19] was used to analyse for the presence of slip at the die wall, for which it is required to find the apparent wall shear rate at controlled values of wall shear stress. Using an experimental setup where the extrusion is controlled via the load frame cross head speed, extrusion pressures were measured for a specified set of velocities used for all three die diameter sets. Having fitted a three parameter power law curve to the data, the apparent wall shear rates corresponding to the specified wall shear stress values required for the Mooney analysis, were interpolated for each die set.

This data was then used to estimate the slip velocity at the die wall. The flow rate of the extrudate is assumed to be due to the superimposition of the bulk material flow rate and the slip flow rate;

$$Q_{tot} = Q_{bulk} + Q_{slip}. \quad 2$$

Writing the flow rates in terms of velocity, the shear rate at the die wall for a Newtonian fluid is given by the first term of the following equation;

$$\frac{8V_{ext}}{D} = \frac{8V_{bulk}}{D} + \frac{8V_{slip}}{D} \quad 3$$

where V_{ext} is the extrudate velocity, V_{bulk} is the velocity of the bulk material and V_{slip} is the slip velocity. The slip velocity can be obtained from the gradient of $8V_{ext}/D$ versus $1/D$ at a given wall shear stress, as indicated by Eq. (3). The first term on the right side of Eq. (3) represents for a Newtonian fluid, the shear rate of the bulk material at the slip interface. To find the true shear rate of the bulk material at the slip interface, a correction for non-Newtonian flow is required.

For pastes made with Newtonian binder systems the slip velocity is typically found to be proportional to the wall shear stress as follows, where β is the slip coefficient.

$$V_{slip} = \beta\tau_w \quad 4$$

For non-Newtonian binder systems the slip velocity is not directly proportional to the wall shear stress, as a result of the binder rheological properties. The application of a power law relationship has successfully been applied in previous studies such as that by Kalyon [14];

$$V_{slip} = \beta\tau_w^n \quad 5$$

where n is a power law exponent which should have a positive value which is dependent upon the binder rheological properties as well as the properties of the bulk material/powder suspension [10,14]. The slip coefficient is itself a function of the slip layer thickness, the flow properties of the binder [14].

Lam et al. [10] showed the slip velocity to be a function of solids loading obtaining a significant improvement in correlation between the slip velocities of pastes of various solids loadings by plotting the slip velocity versus the product of wall shear stress and the square root of solids loading. The following relationship was proposed;

$$V_{slip} = \beta\left(\tau_w\sqrt{\phi}\right)^n. \quad 6$$

Jastrzebski has previously reported capillary rheometry results which propose the slip velocity is inversely proportional to the inverse of the

die radius such that a linear plot could be obtained from the apparent shear rate versus $8/D^2$. However, as critical reviews of this proposed method, it has no physical basis [20]. In situations where the Mooney analysis does not result in a linear plot, the Tikhonov regularization method is reported to have provided improved results [20].

3.4. Velocity profile

For the purposes of finding the velocity profile, the bulk flow properties under shear flow were characterised using the Herschel Bulkley model;

$$\tau_w = \tau_B + K\dot{\gamma}_w^b \quad (7)$$

where τ_w is the wall shear stress, τ_{HB} is the Herschel Bulkley yield shear stress, K is the shear rate coefficient (flow index), b represents the power law exponent and $\dot{\gamma}_w$ is the bulk shear rate at the wall (or the slip layer interface).

The true bulk shear rate of the paste at the wall (slip interface) is obtained by correcting the shear rate at the wall calculated for a Newtonian fluid, $\dot{\gamma}_{bulk}$, taking into account the non-parabolic velocity profile of the paste (attributed to non-Newtonian flow behaviour), referred to as the Weissenberg–Rabinowitsch correction [21];

$$\dot{\gamma}_w = \frac{8V_{ext}}{D}\left[\frac{1}{4}\left(\frac{3 + d\ln\dot{\gamma}_{bulk}}{d\ln\tau_w}\right)\right] \quad (8)$$

where the gradient of the apparent shear rate was obtained by differentiating a quadratic equation fitted to a plot of $\ln\dot{\gamma}_{bulk}$ versus $\ln\tau_w$.

3.5. Relative viscosity predictions

The Krieger–Dougherty equation [22] was used as an empirical expression of the change in shear viscosity or die entry pressure with solids loading;

$$\eta_r = \left(1 - \frac{\phi}{\phi_m}\right)^{-[\eta]\phi_m} \quad (9)$$

where η_r is the relative viscosity and ϕ is the solids packing fraction. A hydrodynamic factor $[\eta]$ of 2.5 was used and maximum (critical) solids loading values (ϕ_m) of 56.5% v/v for the twin roll mixed pastes and 57% v/v for the z-blade mixed pastes were used. The critical solids loading values were obtained using the method previously described by Powell and Blackburn [5]. This method involves extruding pastes of a given powder composition and binder formulation but with varying powder to binder ratios, therefore producing extrusion pressures for pastes with varying solids loadings (solids volume fractions). From this data it is possible to extrapolate to a solids loading where the extrusion pressure tends to infinity, which represents the solids loading of paste that cannot undergo extrusion. It is assumed that such a solids loading represents the maximum solids loading of the paste, where the solid particles are no longer lubricated by the liquid binder and are in direct contact with each other, resulting in interlocked powder particles, preventing deformation of the powder bed.

4. Results

4.1. Paste rheology

The described extrusion rheometry test was carried out for all pastes. Fig. 2 shows a typical Bagley plot of the extrusion pressure data. As indicated by the linear plot, the pastes were well mixed and die land flow was fully developed at the entrance to the die. The data points for the various pastes fit the linear regression curve with an R^2 values ranging between 0.985 and 0.999.

Fig. 2 shows a typical plot of the extrusion pressure versus ram velocity for the three die lengths, where the data is that of a paste with a solids loading of 52.5% v/v. The estimated error of each extrusion pressure data point ranges between 0.5% and 2.5%, based on the standard deviation of extrusion loads measured at a given ram velocity over a ram displacement of at least 5 mm as well as data obtained from at least two batches of the same formulation.

The chart shows a good fit between the experimental data and the Benbow–Bridgwater model curves, the parameters for which are given in Table 3. The high σ_0 parameter indicates a significant die entry yield stress, whereas, there exists no apparent yield stress for the die land flow, as indicated by the zero value for τ_0. This result is consistent with results published by Kalyon which showed concentrated suspensions of particles with a high Peclet number (subject to negligible Brownian motion effects) to have a slip yield stress of zero [14].

4.2. Solids loading

The apparent viscosity (wall shear stress/apparent wall shear rate) and die entry pressure drop were calculated and compared to the predicted trend in viscosity with increasing solids loading. The relative viscosity, which is the ratio of the paste viscosity and the binder viscosity, was obtained using the Krieger–Dougherty equation, refer to Eq. (10). The Krieger–Dougherty equation is not used to predict the paste viscosity at various solids loadings, but for the purpose of comparing the trend in extrusion pressures and apparent viscosities with solids loadings for the two flow regimes, die entry and die land.

Figs. 3 and 4 show the apparent shear viscosities, die entry pressures and predicted relative viscosities at various solids loadings, for pastes mixed using a twin roll mill and a z-blade kneader respectively. As expected from the trends indicated by the Krieger–Dougherty equation, there is an exponential growth in viscosity with increasing solids loading, which is mirrored by the increase in die entry pressure, which of course is independent of slip flow. However for apparent shear viscosities measured for both z-blade and twin roll mill mixed pastes, the trend does not follow that of the Krieger–Dougherty equation. For the twin roll mill pastes a well pronounced plateau in the apparent viscosity exists, with the apparent viscosity at a given shear rate being relatively independent of solids loading above a value 54% v/v, as shown in the upper plot of Fig. 3.

The solids loading of 55.4% v/v was the highest that could be produced with the twin roll mill. Above this maximum solids loading, the paste was not only too dry to adhere effectively to the rollers of the

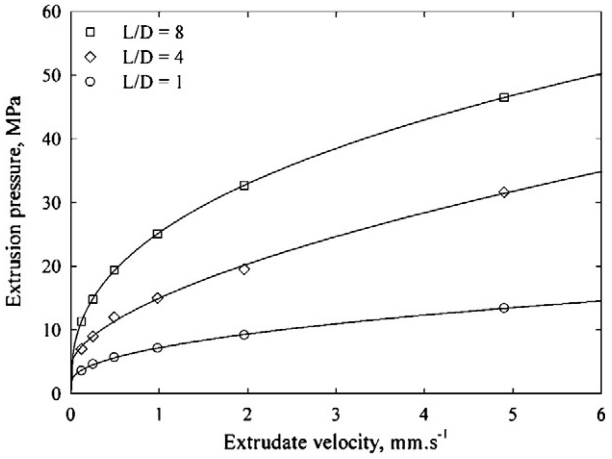

Fig. 2. YSZ extrusion rheometry pressure data, D = 4 mm. Solid line represents the Benbow–Bridgwater model fit. Paste solids loading.

Table 3
Example of Benbow–Bridgwater parameters for YSZ pastes used in this study.

Die entry parameters	σ_0 (MPa)	0.44
	α (MPa (s/m)^m)	37.05
	m (dimensionless)	0.52
Die land parameters	τ_0 (MPa)	0.00
	β (MPa (s/m)^n)	8.90
	n (dimensionless)	0.38

mill, but could also not be extruded at loads below the 100 kN safety limit set on the load frame.

Referring to Fig. 4, one can observe a similar plateau in apparent velocity as seen for the twin roll mill mixed pastes, but in this case a higher solids loading could be produced. This paste exhibits a sudden and significant increase in apparent shear viscosity indicating the end of the plateau region. Again, the die entry pressure shows a trend similar to that of the Krieger–Dougherty relationship.

This observed plateau in the die land extrusion pressure/apparent viscosity lies within a range of solids loadings which according to results reported by Pusey and van Megen [23] for suspensions of mono-sized spherical particles exhibit crystal or glass phase properties. The crowding of particles in this glass or crystal like state inhibits Brownian motion of the solid particles and so slip flow is promoted. As the powder used was not composed of mono-sized spherical particles one would expect a lower maximum packing density and therefore would expect the glass transition to take place at a lower solids loading than the value quoted by Pusey and van Megen.

4.3. Wall slip

Mooney analysis was performed on two paste formulations, each with a different solids loading, 52.5% v/v and 55.4% v/v. Both pastes were mixed using the twin roll mill. The purpose of this analysis is to confirm if the observed plateau in die land extrusion pressures is due to slip flow behaviour. The solids loadings 52.5% v/v twin roll milled paste sits outside of this plateau, whereas the higher solids loading 55.5% v/v, the maximum solids loading tested, represents a solids loading that sits within the observed die land extrusion pressure plateau.

The interpolated wall shear stress data obtained for the paste with a 52.5% v/v solids loading is plotted as a function of the inverse of the die diameter in Fig. 5, showing a good fit between the linear regression and the data, with positive values for the intercept at the y-axis as should be the case for the Mooney analysis to be applicable.

Figs. 6 and 7 shows the velocity profiles of the paste in a 6 mm diameter die at various wall shear stresses. These profiles are based upon the estimated slip velocities obtained from the Mooney analysis, and the rheological parameters of the bulk shear flow behaviour, obtained using the Herschel–Bulkley equation (Eq. (8)), the parameters for which are provided in Table 4. From Figs. 6 and 7 it can be seen that over this range of solids loadings the slip flow is

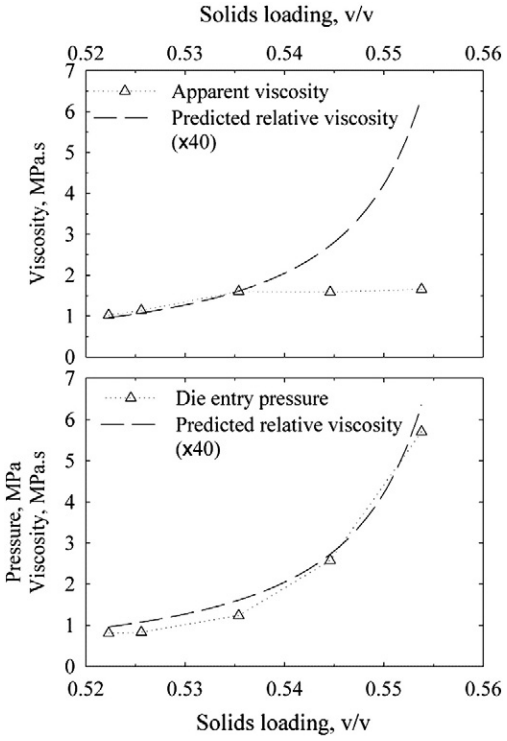

Fig. 3. Apparent shear viscosities and die entry pressures for twin roll mixed pastes at various solids loadings. Critical solids loading of 56.5% v/v. Relative viscosity predictions obtained using Dougherty–Krieger equation. $V_{ext} = 5$ mm.s^{-1} and $D = 4$ mm.

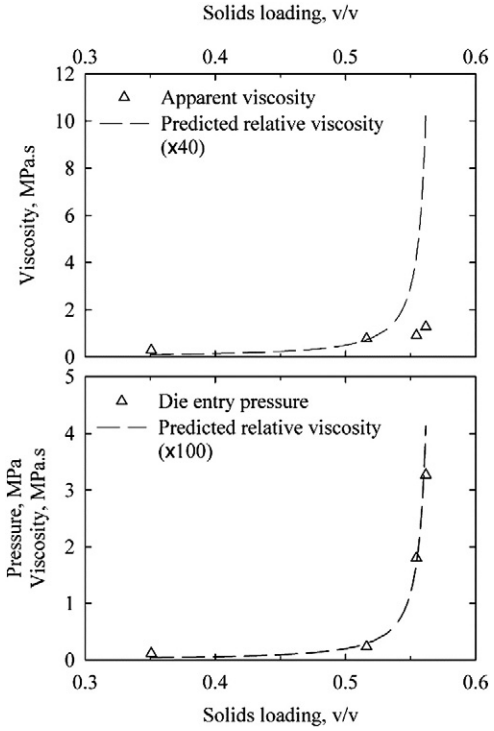

Fig. 4. Apparent shear viscosities and die entry pressures for z-blade mixed pastes at various solids loadings. Critical solids loading of 57% v/v. Relative viscosity predictions obtained using Dougherty–Krieger equation. $V_{ext} = 5$ mm.s^{-1} and $D = 4$ mm.

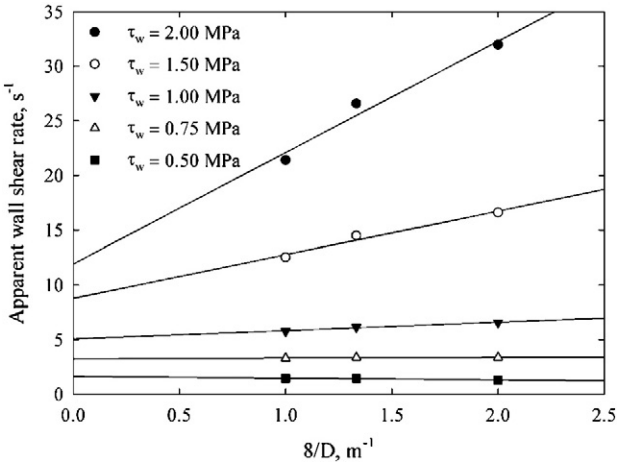

Fig. 5. Mooney plot of YSZ extrusion rheometry data.

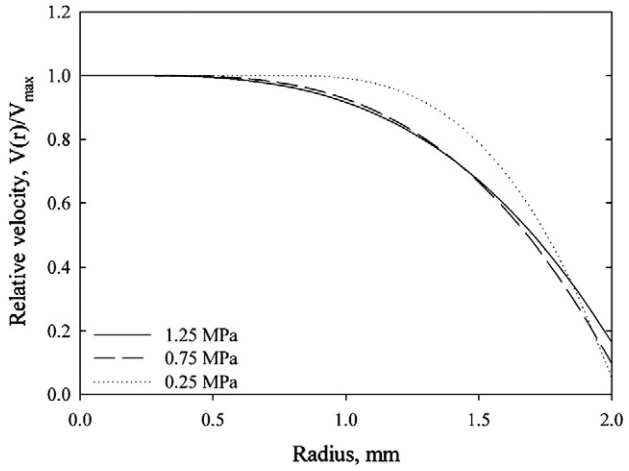

Fig. 6. Velocity profile of paste with 52.5% v/v solids loading at various wall shear stresses.

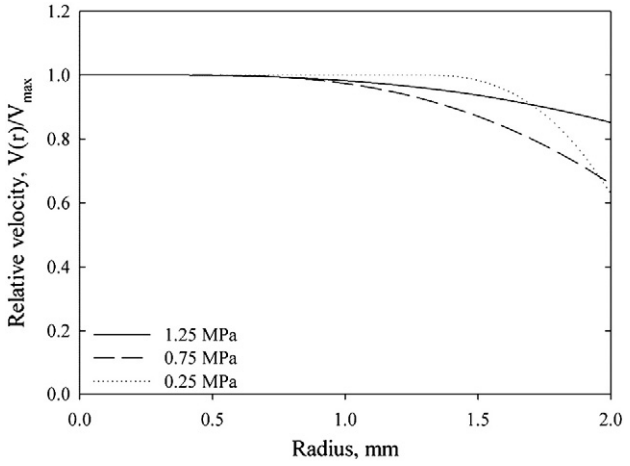

Fig. 7. Velocity profiles of a paste with a 55.4% v/v solids loading at various wall shear stresses.

significantly more dominant for the paste with a solids loading of 55.4%, which also has more uniform velocity profiles as is desirable in co-extrusion processes. This greater uniformity of the velocity profile is a result of a more significant slip velocity relative to the maximum velocity as well as a higher yield stress τ_0.

Fig. 8 shows a log–log scale of wall shear stress versus the slip velocity for pastes with 52.5% and 55.5% solids loadings. These results are consistent with those reported by Lam et al. [10] which show an increase in slip velocity with solids loading at constant wall shear stress, which as stated by these authors indicates that the relationship between slip velocity and solids loading is not adequately described by wall shear stress alone. The parameters for Eq. (5), the coefficient β and wall shear stress exponent, $1/n$, are given in Table 5, where n is the power law index of the binder in the slip layer. The increase in β with solids loading is consistent with results reported by Jana et al. [13] and Ballesta et al. [12].

Lam et al. [10] correlated the slip velocities of pastes with various solids loadings by plotting the slip velocity as a function of wall shear stress and the solids loading. As can be seen from Fig. 8 no significant change in the correlation between the two data sets was achieved. The standard error of estimate for the power law regression curve fitted to the V_{slip} versus τ_w data is 0.55, compared to that of the V_{slip} versus $\tau_w\sqrt{\phi}$ plot where the standard error is 0.67.

5. Discussion

Formulating a paste within the range of solids loadings where slip flow is dominant provides a benefit in the co-extrusion of pastes such as in the manufacture of micro-tubular solid oxide fuel cells [6]. In such applications where the relative feed rates of the streams are fixed such that they cannot be controlled separately, the promotion of plug flow due to wall slip is necessary to obtain a stable laminate geometry.

Figs. 3, 4 and 10 show that for a narrow range of solids loadings (approximately 0.54 to 0.56), at an extrusion velocity of 5 mm.s^{-1}, the die land extrusion pressure is relatively independent of solids loading. This effect is observed for z-blade and twin roll milled pastes, mixers which have very different mixing mechanisms, implying that it is not a result of the mixing process and a change in its performance with solids loading.

Figs. 8 and 9 show that the slip velocity is a function of the wall shear stress by means of a power law relationship, such that the higher the wall shear stress the higher the slip velocity, which is expected in light of the shear thinning behaviour of the binder.

The higher slip velocities observed for the higher solids loading paste are conducive with the results shown in Fig. 9. However the differences in slip velocity at a given wall shear stress cannot be explained in terms of solid loading by application of the relationship proposed by Lam et al. [10].

Kalyon [14] presented an equation that presents the slip coefficient attributed to solids depletion slip flow as being a function of the slip, δ, the flow consistency parameter of the binder, m, slip layer and the power law index of the binder slip layer, n, according to the following equation;

$$\beta = \frac{\delta}{m^{1/n}}. \qquad 10$$

As the pastes of different solids loadings were made using the same binder system, one might assume the power law index, n, and the consistency index, m, the same for all pastes tested in this study. However according to the results presented in Table 5, it is the apparent decrease in the $1/n$ term that leads to the increase in the slip coefficient, which in turn leads to the increase in the slip velocity. This implies that n is not only a function of the binder rheological properties but also the solids loading and powder properties.

Assuming a constant value for the consistency index, m, according to Eq. (10),in order to the achieve the observed increase in the slip coefficient, an approximately 50% decrease in the slip layer thickness, δ, would need to take place. Results from previous studies including results published by Kalyon [14]have shown an inverse relationship between the solids loading and slip layer thickness. Experimental data was fitted to the following equation, where D_p is the harmonic mean diameter.

$$\frac{\delta}{D_p} = 1 - \frac{\phi}{\phi_m}$$

Table 4
Herschel Bulkley parameters for pastes with solids loadings of 52.5% and 55.5%.

Solids loading	52.5% v/v	55.5% v/v
τ_{HB}	0.0931	0.1620
K	0.2830	1.376
b	0.5102	0.6592

Table 5
Slip parameters for pastes with 52.5% and 55.5% solids loadings calculated using Eq. (5).

Solids loading %	β(MPa^{-n} m. s^{-1})	$1/n$
52.5	0.9	3.5
55.5	1.7	2.2

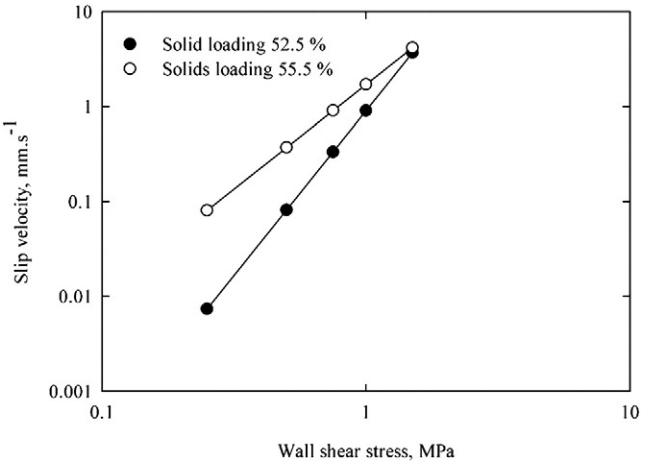

Fig. 8. Log–log scale plot of wall shear stress versus slip velocity for pastes with solids loadings of 52.5% and 55.5%.

Assuming a maximum packing density of 56.5% for the z-blade mixed pastes, as approximated from the extrusion pressure results, then using the above equation one would expect a 75% reduction in the slip layer thickness with an increase in solids loading from 52.5 to 56.5%.

6. Conclusions

The rheological properties and thus the extrusion pressure of pastes are highly sensitive to the volume fraction of solids. The change in die entry extrusion pressure with solids loading follows a similar trend to that given by the Krieger–Dougherty equation. Regarding the change in die land extrusion flow behaviour with solids loading, the results shown indicate that for twin roll milled pastes with solids loadings below 54% v/v, the ceramic pastes exhibit relatively little slip flow. For pastes with a solids loading above approximately 53/54% v/v and below the critical solids loading of approximately 56/57% v/v, the apparent shear viscosity of the paste was relatively independent of the solids loading. These results show some similarity to those reported by Ballesta et al. [12] where a significant increase in slip flow behaviour was observed in the transition from a viscous paste to a glass phase paste and the onset of plug flow behaviour.

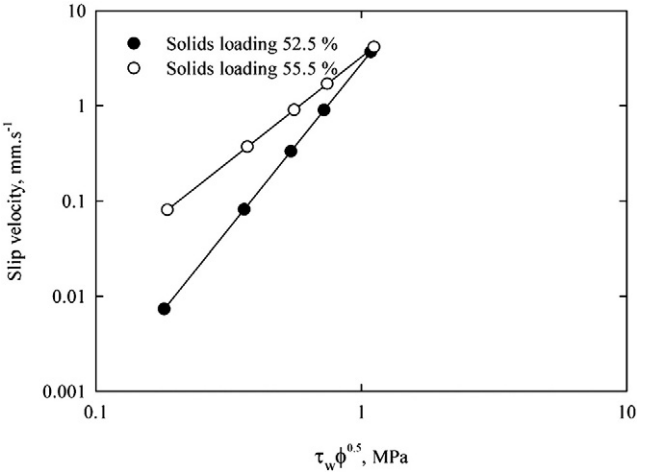

Fig. 9. Log–log scale plot of the product of wall shear stress and the square root of solids loading versus the slip velocity for pastes with solids loadings of 52.5% and 55.5%.

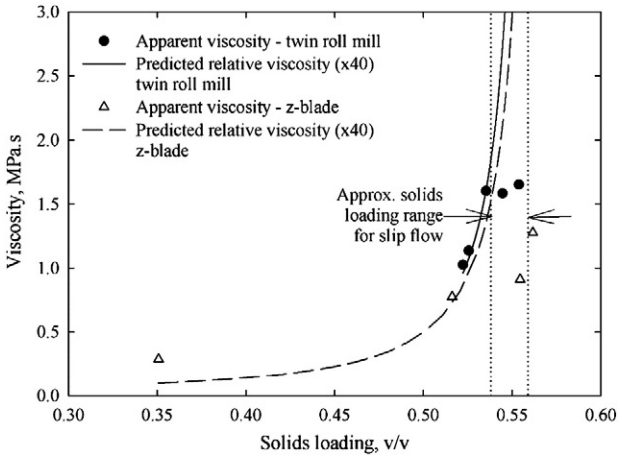

Fig. 10. Chart of apparent shear viscosity for z-blade and twin roll mill mixed pastes with varying solids loading and the predicted trend in relative viscosity calculated from the Krieger–Dougherty equation. Dotted vertical lines represent the approximate limits for solids loadings, where paste die land flow is dominated by slip.

References

[1] Z. Liang, S. Blackburn, Design and characterisation of a co-extruder to produce trilayer ceramic tubes semi-continuously, Journal of the European Ceramic Society 21 (7) (2001) 883–892.
[2] Z. Liang, S. Blackburn, Analysis of crack development during processing of laminated ceramic tubes, Journal of Materials Science 37 (19) (2002) 4227–4233.
[3] W. Zhang, J. Xie, C. Wang, Fabrication of multilayer 316L/PSZ gradient composite pipes by means of multi-billet extrusion, Materials Science and Engineering A 382 (1–2) (2004) 371–377.
[4] Z. Chen, K. Ikeda, T. Murakami, T. Takeda, J.-X. Xie, Fabrication of composite pipes by multi-billet extrusion technique, Journal of Materials Processing Technology 137 (1–3) (2003) 10–16.
[5] J. Powell, S. Blackburn, The unification of paste rheologies for the co-extrusion of solid oxide fuel cells, Journal of the European Ceramic Society 29 (5) (2009) 893–897.
[6] J. Powell, S. Blackburn, Co-extrusion of multilayered ceramic micro-tubes for use as solid oxide fuel cells, Journal of the European Ceramic Society 30 (14) (2010) 2859–2870.
[7] H.A. Barnes, A review of the slip (wall depletion) of polymer solutions, emulsions and particle suspensions in viscometers: its cause, character, and cure, Journal of Non-Newtonian Fluid Mechanics 56 (3) (1995) 221–251.
[8] D.I. Wilson, S.L. Rough, Exploiting the curious characteristics of dense solid–liquid pastes, Chemical Engineering Science 61 (13) (2006) 4147–4154.
[9] A.U. Khan, B.J. Briscoe, P.F. Luckham, Evaluation of slip in capillary extrusion of ceramic pastes, Journal of the European Ceramic Society 21 (4) (2001) 483–491.
[10] Y.C. Lam, Z.Y. Wang, X. Chen, S.C. Joshi, Wall slip of concentrated suspension melts in capillary flows, Powder Technology 177 (3) (2007) 162–169.
[11] J. Gotz, D. Muller, H. Buggisch, C. Tasche-Lara, NMR flow imaging of pastes in steady-state flows, Chemical Engineering and Processing 33 (5) (1994) 385–392.
[12] P. Ballesta, G. Petekidis, L. Isa, W.C.K. Poon, R. Besseling, Wall slip and flow of concentrated hard-sphere colloidal suspensions, Journal of Rheology 56 (5) (2012) 1005–1037.
[13] S.C. Jana, B. Kapoor, A. Acrivos, Apparent wall slip velocity coefficients in concentrated suspensions of noncolloidal particles, Journal of Rheology 39 (6) (1995) 1123–1132.
[14] D.M. Kalyon, Apparent slip and viscoplasticity of concentrated suspensions, Journal of Rheology 49 (3) (May/June 2005) 621–640.
[15] P. Ballesta, R. Besseling, L. Isa, G. Petekidis, W.C.K. Poon, Slip and flow of hard-sphere colloidal glasses, Physical Review Letters 101 (25) (2008) 258301.
[16] P.J.A. Hartman Kok, S.G. Kazarian, B.J. Briscoe, C.J. Lawrence, Effects of particle size on near-wall depletion in mono-dispersed colloidal suspensions, Journal of Colloid and Interface Science 280 (2) (2004) 511–517.
[17] D.R. Foss, J.F. Brady, Structure, diffusion and rheology of Brownian suspensions by Stokesian Dynamics simulation, Journal of Fluid Mechanics 407 (2000) 167–200.
[18] J.J. Benbow, J. Bridgwater, Paste Flow and Extrusion, Clarendon Press, Oxford, 1993.
[19] M. Mooney, Explicit formulas for slip and fluidity, Journal of Rheology 2 (2) (1931) 210–222.
[20] P.J. Martin, D.I. Wilson, A critical assessment of the Jastrzebski interface condition for the capillary flow of pastes, foams and polymers, Chemical Engineering Science 60 (2) (2005) 493–502.
[21] R. Eisenschitz, B. Rabinowitsch, K. Weissenberg, Mitteil Deutsch, Materialspruefungsamt, Sonderheft, 9(91), 1929.
[22] I.M. Krieger, T.J. Dougherty, A mechanism for non-Newtonian flow in suspensions of rigid spheres, Transactions of the Society of Rheology 3 (1959) 137–152.
[23] P.N. Pusey, W. van Megen, Phase behaviour of concentrated suspensions of nearly hard colloidal spheres, Nature 320 (6060) (1986) 340–342.